THE JOURNAL OF BIOLOGICAL CHEMISTRY VOL. 286, NO. 21, pp. 18414–18425, May 27, 2011

Age-dependent Accumulation of Soluble Amyloid β (Aβ) Oligomers Reverses the Neuroprotective Effect of Soluble Amyloid Precursor Protein-α (sAPPα) by Modulating Phosphatidylinositol 3-Kinase (PI3K)/Akt-GSK-3β Pathway in Alzheimer Mouse Model*[S]

Received for publication, December 8, 2010, and in revised form, March 4, 2011 Published, JBC Papers in Press, April 1, 2011, DOI 10.1074/jbc.M110.209718

Sebastian Jimenez[‡§¶1,2], Manuel Torres[‡§¶1,2], Marisa Vizuete[‡§¶], Raquel Sanchez-Varo[§‖2], Elisabeth Sanchez-Mejias[§‖3], Laura Trujillo-Estrada[§‖3], Irene Carmona-Cuenca[‡§¶], Cristina Caballero[‡§¶], Diego Ruano[‡§¶], Antonia Gutierrez[§‖], and Javier Vitorica[‡§¶4]

From the [‡]Departamento Bioquímica y Biología Molecular, Facultad de Farmacia, Universidad de Sevilla, 41012 Sevilla, the [‖]Departamento Biología Celular, Genética y Fisiología, Facultad de Ciencias, Universidad de Málaga, 29071 Málaga, the [§]Centro de Investigación Biomédica en Red Sobre Enfermedades Neurodegenerativas, 41013 Sevilla, and the [¶]Instituto de Biomedicina de Sevilla-Hospital Universitario Virgen del Rocío/Consejo Superior de Investigaciones Científicas/Universidad de Sevilla, 41013 Sevilla, Spain

Neurotrophins, activating the PI3K/Akt signaling pathway, control neuronal survival and plasticity. Alterations in NGF, BDNF, IGF-1, or insulin signaling are implicated in the pathogenesis of Alzheimer disease. We have previously characterized a bigenic PS1×APP transgenic mouse displaying early hippocampal Aβ deposition (3 to 4 months) but late (17 to 18 months) neurodegeneration of pyramidal cells, paralleled to the accumulation of soluble Aβ oligomers. We hypothesized that PI3K/Akt/GSK-3β signaling pathway could be involved in this apparent age-dependent neuroprotective/neurodegenerative status. In fact, our data demonstrated that, as compared with age-matched nontransgenic controls, the Ser-9 phosphorylation of GSK-3β was increased in the 6-month PS1×APP hippocampus, whereas in aged PS1×APP animals (18 months), GSK-3β phosphorylation levels displayed a marked decrease. Using N2a and primary neuronal cell cultures, we demonstrated that soluble amyloid precursor protein-α (sAPPα), the predominant APP-derived fragment in young PS1×APP mice, acting through IGF-1 and/or insulin receptors, activated the PI3K/Akt pathway, phosphorylated the GSK-3β activity, and in consequence, exerted a neuroprotective action. On the contrary, several oligomeric Aβ forms, present in the soluble fractions of aged PS1×APP mice, inhibited the induced phosphorylation of Akt/GSK-3β and decreased the neuronal survival. Furthermore, synthetic Aβ oligomers blocked the effect mediated by different neurotrophins (NGF, BDNF, insulin, and IGF-1) and sAPPα, displaying high selectivity for NGF. In conclusion, the age-dependent appearance of APP-derived soluble factors modulated the PI3K/Akt/GSK-3β signaling pathway through the major neurotrophin receptors. sAPPα stimulated and Aβ oligomers blocked the prosurvival signaling. Our data might provide insights into the selective vulnerability of specific neuronal groups in Alzheimer disease.

The molecular mechanisms underlying the selective neurodegeneration in Alzheimer disease (AD)[5] remain unclear. Amyloid-β (Aβ) peptides, proteolytically excised from the amyloid precursor protein (APP), are considered the primary pathological agents in AD. However, their precise modes of action, toxic conformational forms, and molecular targets are still controversial (for review see Ref. 1). Transgenic mouse models, overexpressing mutated forms of human APP, are widely used to study AD pathogenesis. These models develop extensive Aβ deposition in the disease-vulnerable brain regions (such as hippocampus); however, neurons are well protected until late ages. The factors and pathways maintaining neuronal integrity at young/middle ages in these AD models and those inducing neurodegeneration in the aged animals remains to be defined.

NGF, BDNF, IGF-1, and insulin are trophic factors critical for neuronal survival and plasticity, underlying memory, and learning (2–4) and could be implicated in AD development. Changes in growth factor expression and distribution, as well in their receptors (TrkA, TrkB, p75NTR, IGF-1R, and insulin-R), have been reported in AD and AD models (5). In fact, it has been suggested that the imbalance between NGF, its precursor proNGF, and the high (TrkA) and low (p75NTR) affinity NGF receptors seems to be a crucial factor underlying neurodegen-

* This work was supported in part by Grants PS09/00151 (to J. V.), PS09/00099 (to A. G.), and PS09/00848 (to D. R.) from the Fondo de Investigación Sanitaria (Instituto de Salud Carlos III, Spain) and by Grants CTS-4795 (to J. V.) and SAS PI-0496/2009 (to A. G.) from Junta de Andalucía (Spain).

[S] The on-line version of this article (available at http://www.jbc.org) contains supplemental Figs. 1–4.

[1] Both authors contributed equally to this work.

[2] Recipient of a contract from the Centro de Investigación Biomédica en Red Sobre Enfermedades Neurodegenerativas.

[3] Recipient of a Ph.D. fellowship from the Formación de Proferorado Universitario (FPU) Program (Spain).

[4] To whom correspondence should be addressed: Dept. of Bioquímica y Biología Molecular, Facultad de Farmacia, Universidad de Sevilla, 41012 Sevilla, Spain. Tel.: 34-954556670; E-mail: vitorica@us.es.

[5] The abbreviations used are: AD, Alzheimer disease; APP, amyloid precursor protein; sAPP, soluble APP; Aβ, amyloid β-protein; tg, transgenic; Tricine, *N*-[2-hydroxy-1,1-bis(hydroxymethyl)ethyl]glycine; ADDL, Aβ-derived diffusible ligand.

eration in AD (6, 7). Furthermore, defects in IGF-1R and insulin-R signaling are associated with amyloid plaque and neurofibrillary tangle pathology (8). In this sense, it has been reported that insulin resistance, central to type II diabetes, was implicated in the pathogenesis of AD. Alterations in IGF-1R, insulin-R, and IRS-1/2 in AD are implicated in insulin resistance (9). In fact, AD has been considered as a brain-specific "type III diabetes" (10, 11). Insulin administration facilitates memory in patients with AD (12), and IGF-1 is protective against the development of Aβ pathology (13). However, the mechanisms implicated in the Aβ-mediated insulin resistance are still unknown.

Trophic factors promote neuronal survival largely through the PI3K/Akt signaling pathway (14). After activation, phospho-Akt phosphorylates and inhibits the glycogen synthase kinase-3β (GSK-3β). The "GSK3 hypothesis of AD" (15) proposed that the overactivity of GSK-3β accounts for several features of this pathology such as memory impairment, Tau phosphorylation, increased amyloid production, microglia-mediated inflammation, and neuronal death. In fact, GSK-3β mediates the hyper-phosphorylation of Tau (16) and produces impairments in learning and memory by preventing the induction of long term potentiation (17). GSK-3β activity also is critical for inflammatory cell differentiation, migration, and secretion of pro-inflammatory cytokines (18), so it could potentially heighten microglia-mediated inflammatory responses in the local vicinity of Aβ plaques. Moreover, GSK-3β modulates key steps of the major apoptotic signaling pathways (the mitochondrial intrinsic apoptotic and the death receptor-mediated extrinsic apoptotic pathways) (19).

Increasing evidence suggests that the PI3K/Akt/GSK-3β signaling pathway is directly impacted by Aβ exposure and is altered in AD brains. In this sense, soluble (or diffusible) Aβ oligomers (putative toxic agents in AD) (20, 21) have been associated with Tau hyperphosphorylation (22), inhibition of long term potentiation, disruption of memory, loss of dendritic spine density (23), neuronal death (24, 25), and neurotoxic inflammatory response (26). Furthermore, Aβ oligomers have been shown to modulate the expression and density of insulin receptors through the modulation of the PI3K/Akt pathway (27), and alterations in the levels of phosphorylated Akt substrates have been reported in AD patients (28).

In this study, we have addressed the possible age-dependent variations in the GSK-3β phosphorylation in our PS1×APP tg model. This model developed early Aβ (3 to 4 months) plaques (29–31) but late (17 to 18 months) hippocampal neuronal degeneration, paralleled with the accumulation of soluble Aβ oligomers (26). The molecular changes that drive to this apparent age-dependent protective/degenerative neuronal condition are still unresolved. We hypothesized that the PI3K/Akt/GSK-3β signaling pathway could be involved. Using *in vivo* and *in vitro* assays, we report that natural and synthetic Aβ oligomers, acting through growth factor receptors, inhibit the prosurvival signaling PI3K/Akt/GSK-3β. Moreover, at early ages, despite the Aβ plaques, soluble APPα, acting through IGF-1 and insulin receptors, activated the prosurvival PI3K-Akt-GSK-3β pathway that might account for the lack of neurodegeneration in most transgenic models at these ages.

EXPERIMENTAL PROCEDURES

Antibodies—A11 and 6E10 antibodies were purchased from Invitrogen and Signet Laboratories, respectively. Anti-soluble APPα was provided by Immuno-Biological Laboratories. Anti-phospho-GSK-3β (Ser-9); phospho-Akt (Ser-473); phospho-Akt (Thr-308); phospho-IGF1 receptor β (Tyr-1135/1136); pTrkA-B (TrkA, Tyr-674/675; TrkB, Tyr-706/707) were from Cell Signaling Laboratory. Anti-phospho-insulin receptor (Tyr-1150/1151) was purchased from Millipore. Monoclonal anti-human PHF-Tau (Clone AT100) was purchased from Innogenetics. Anti-phospho- and total β-catenin antibodies were from Cell Signaling Laboratory and Abcam, respectively. Anti-β-actin was purchased from Sigma.

Transgenic Mice—The generation and initial characterization of the $PS1_{M146L}$×APP_{751sl} (PS1×APP) tg mice has been reported previously (29). This double tg mice (C57BL/6 background) were generated by crossing homozygotic $PS1_{M146L}$ mice with heterozygotic Thy1-APP751SL mice (all tg mice were provided by Transgenic Alliance, IFFA Credo, Lyon, France). Mice represented F10–F15 offspring of heterozygous tg mice. Only male mice were used in this work. Age-matched $PS1_{M146L}$ and nontransgenic (WT) male mice of the same genetic background (C57BL/6) were used as controls.

For glucose determination, the anesthetized (sodium pentobarbital; 60 mg/kg) animals were bled (50 μl) from the tail. The glucose levels were similar between ages and genotypes (in mM: 6.4 ± 1.4, 5.4 ± 1.2; 7.3 ± 1.2 and 6.5 ± 1.4, $n = 7$, for 6 or 18 months, WT and PS1×APP, respectively). After bleeding, the mice were killed by decapitation, and both hippocampi were dissected, frozen in liquid N_2, and stored at −80 °C until use. All animal experiments were performed in accordance with the guidelines of the Committee of Animal Research of the University of Seville (Spain) and the European Union Regulations.

RNA and Total Protein Extraction—Total RNA was extracted using the Tripure™ isolation reagent (Roche Applied Science) as described previously (30, 31).

The contaminating DNA in the RNA samples was removed by incubation with DNase (Sigma) and confirmed by PCR analysis of total RNA samples prior to reverse transcription (RT). After isolation, the integrity of the RNA samples was assessed by agarose gel electrophoresis. The yield of total RNA was determined by measuring the absorbance (260/280 nm) of ethanol-precipitated aliquots of the samples. The recovery of RNA was comparable in all groups (1.2–1.5 μg/mg of tissue). The protein pellets, obtained using the Tripure™ isolation reagent, were resuspended in 4% SDS and 8 M urea in 40 mM Tris-HCl, pH 7.4, and rotated overnight at room temperature (30, 31).

Retrotranscription and Real Time RT-PCR—The retrotranscription (RT) was done using random hexamers, and 3 μg of total RNA as template and high capacity cDNA archive kit (Applied Biosystems) following the manufacturer recommendations (30, 31). For real time RT-PCR, each specific gene product was amplified using commercial TaqMan™ probes, following the instructions of the manufactured (Applied Biosystems), using an ABI Prism 7000 sequence detector (Applied Biosystems). For each assay, a standard curve was first constructed, using increasing amounts of cDNA. In all cases, the

slope of the curves indicated optimal PCR conditions (slope 3.2–3.4). The cDNA levels of the different mice were determined using two different housekeepers (*i.e.* GAPDH and β-actin). The amplification of the housekeepers was done in parallel with the gene to be analyzed. Similar results were obtained using both housekeepers. Thus, the results were normalized using only the GAPDH expression.

Independently of the gene analyzed, the results were always expressed using the comparative *Ct* method, following Bulletin 2 from Applied Biosystems. As a control condition, we selected 6-month-old WT mice. In consequence, the expression of all tested genes, for all ages and mouse types, was referenced to the expression levels observed in 6-month-old WT mice.

Aβ42 Peptide Preparation—To prepare the Aβ42 peptides, we allowed synthetic lyophilized Aβ(1–42) peptide (human sequence, Anaspec) to equilibrate, at 20–23 °C, for 30 min before it was resuspended and diluted to 1 mM in hexafluoro-2-propanol. After evaporation, peptide films were dried in a Speed vacuum and stored at −40 °C. Peptide films were resuspended to 5 mM in dimethyl sulfoxide (DMSO) for 10 min. To form the ADDLs (32), we diluted the 5 mM DMSO solution to 100 μM in cold PBS, vortexed for 30 s, and incubated overnight at 4 °C. Before use, the Aβ/PBS solution was further diluted in culture media. The presence of ADDLs was tested by Western blots using 6E10 (data not shown).

To form the monomers, immediately before use, we diluted the 5 mM DMSO solution in PBS (to a final concentration of 100 μM), following by ultrafiltration through 5-kDa cutoff device (Vivaspin 2, Sartorius Biolab Products). The presence of the monomeric Aβ42 peptide (4.5 kDa) was verified by Western blots (data not shown).

Soluble Protein Extraction (Soluble Fractions) and Immunoprecipitation—The soluble fractions were obtained by ultracentrifugation of the homogenates as described previously (26, 33). Briefly, tissue samples were homogenized (using a Dounce homogenizer) in cold isotonic buffer (0.32 M sucrose, 1 mM EDTA, 1 mM EGTA, 20 mM Tris-HCl, pH 7.5, containing a mixture of protease and phosphatase inhibitors, Sigma) and ultracentrifuged (Optima™ MAX Preparative Ultracentrifuge, Beckman Coulter) at 120,000 × *g*, 4 °C, during 60 min. Immediately after centrifugation, the samples were aliquoted and stored at −81 °C until use. The protein content in the soluble fractions was determined by Lowry. To diminish the potential inter-individual variability, the S1 fractions from four different mice, for each age and genotype, were pooled.

For immunoprecipitation experiments, 50 μg of soluble proteins were incubated, overnight at 4 °C with continuous shaking, with A11 antibody, previously adsorbed to protein G-Sepharose or protein A-Sepharose beads (Sigma) (2 μg of purified antibody/20 μg of protein G- or A-Sepharose) in the presence of protease inhibitors (Roche Applied Science) in a final volume of 500 μl of TBS. Immunobeads were isolated by centrifugation and washed three times in cold TBS. Finally, the immunoprecipitated proteins were eluted using 20 μl of Laemmli's buffer and analyzed by Western blots.

For *in vitro* experiments, the soluble fractions from the different mice and ages were thawed immediately before use, diluted with DMEM (without FBS), sterilized by filtration (through 0.22-μm filters, Millipore), and added to cell cultures. For each experiment, duplicate wells were stimulated under the same experimental conditions.

The immunodepletion experiments were done basically as described previously (26, 34). Briefly, 50 μg of protein from soluble fractions from 6- and 18-month-old PS1×APP mice (n = 3/age) were subjected to three sequential incubations (8–12 h at 4 °C) with either 6E10 (5 μg) protein G-Sepharose or A11 (5 μg) protein A-Sepharose immunocomplexes. After immunodepletion, the soluble fractions were used for *in vitro* stimulation (see below). As control, the different soluble fractions were sequentially incubated with either protein G-Sepharose or protein A-Sepharose and tested, in parallel experiments, with the immunodepleted samples.

Western Blot and Dot Blot—Western blots were performed as described previously (34). Briefly, 10–20 μg of protein from the different samples were loaded on 16% SDS-Tris-Tricine-PAGE and transferred to nitrocellulose (Hybond-C Extra, Amersham Biosciences). Alternatively, the immunoprecipitated samples were electrophoresed on 12% SDS-Tris glycine.

After blocking, the membranes were incubated overnight, at 4 °C, with the appropriate antibody. The membranes were then incubated with anti-mouse horseradish peroxidase-conjugated secondary antibody (Dako, Denmark) at a dilution of 1:8000. The blots were developed using the ECL-plus detection method (Amersham Biosciences).

Dot blots were done as described previously (26, 34). One μg of protein from the different soluble fractions were directly applied to dry nitrocellulose in a final volume of 2 μl. Blots were air-dried, blocked for 1 h, and incubated overnight at 4 °C, with either Nu-1 (courtesy of Dr. W. Klein; 1 μg/ml) or A11 (1:5000 dilution, BIOSOURCE) antibodies. After the incubation, the blots were washed and visualized as described above.

For quantification, the scanned (Epson 3200) images were analyzed using the PCBAS program. In each experiment, the intensity of bands from WT mice and/or experimental conditions were averaged and considered as 1 relative unit. Data were always normalized by the specific signal observed in 6-month-old WT group or negative control for "*in vitro*" experiments.

Tissue Preparation—After deep anesthesia with sodium pentobarbital (60 mg/kg), 6- and 18-month-old control (WT) and PS1×APP tg male mice (n = 4/age/genotype) were perfused transcardially with 0.1 M phosphate-buffered saline (PBS), pH 7.4, followed by 4% paraformaldehyde, 75 mM lysine, 10 mM sodium metaperiodate in 0.1 M phosphate buffer (PB), pH 7.4. Brains were then removed, post-fixed overnight in the same fixative at 4 °C, cryoprotected in 30% sucrose, sectioned at 40 μm thickness in the coronal plane on a freezing microtome, and serially collected in wells containing cold PBS and 0.02% sodium azide. All animal experiments were approved by the Committee of Animal Use for Research of the Malaga University (Spain) and the European Union Regulations.

Immunohistochemistry—Coronal free-floating brain sections (40 μm thick) from 6-and 18 month-old control (WT) and PS1×APP mice were processed simultaneously for phospho-GSK-3β immunolabeling in the same solutions and conditions to prevent processing variables. Sections were first treated with 3% H_2O_2, 3% methanol in PBS and with

avidin-biotin blocking kit (Vector Laboratories, Burlingame, CA) and then incubated overnight at room temperature with rabbit anti-GSK-3β (phospho-Ser-9) antibody (dilution 1:100, Abcam ab30619).

The tissue-bound primary antibody was detected by incubating with the corresponding biotinylated secondary antibody (1:500 dilution, Vector Laboratories) and then followed by streptavidin-conjugated peroxidase (Sigma) diluted 1:2000. The reaction was visualized with 0.05% 3,3′-diaminobenzidine tetrahydrochloride (Sigma), 0.03% nickel ammonium sulfate, and 0.01% hydrogen peroxide in PBS. Sections were then mounted on gelatin-coated slides, air-dried, dehydrated in graded ethanols, cleared in xylene, and coverslipped with DPX (BDH) mounting medium. Specificity of the immune reaction was controlled by omitting the primary antiserum.

N2a and Primary Neuronal Cultures—N2a cells were plated at 25,000 cells/cm^2 and cultured in high glucose DMEM/OptiMEM (50–50%) supplemented with 2 mM glutamine and 5% fetal bovine serum (PPA Co.) in the presence of penicillin and streptomycin (100 units/ml and 0.01 mg/ml, respectively). For stimulation experiments, the medium was change to high glucose DMEM and serum-deprived for 12 h. The cells were stimulated using 5% fetal bovine serum, 100 nM IGF-1 (Sigma), 100 nM insulin (Sigma), 10 nM NGF-β (Sigma), or 25 nM sAPPα (Sigma) in the presence or absence of ADDLs (ranging from 0.01 to 2 μM; estimated from the initial Aβ42 concentration used for oligomerization; we are aware that the ADDL concentration could be underestimated). After stimulation, the proteins were isolated and analyzed as described above.

Primary neuronal cultures were done essentially as described previously (27). Briefly, embryonic E18–20 or postnatal P1 brains were dissected and treated, for 5 min, with trypsin/DMEM/EDTA medium (BioWhittaker, Cambrex, Belgium). The treatment was stopped using complete DMEM plus 10% FBS, and the cells were mechanically dissociated. After mechanical dissociation, the debris was eliminated by filtration (40 μm, Falcon), and the cells were seeded (at a density of 60,000 cells/ml) in Neurobasal medium plus B27 supplemental (containing glutamine, 1% penicillin/streptomycin and gentamycin) on poly-D-lysine (Sigma)-treated Nunc 12- or 96-well plates. The cells were cultured at 37 °C, in humidified 5% CO_2, 95% atmosphere. Medium was half-replaced every 4 days. After 13–15 days in culture, the cultures were treated with different concentrations (ranging from 0.01 to 2 μM) of ADDLs (prepared as described above) or different concentrations (ranging from 0.27 to 54 nM) of sAPPα. The cells were then incubated for 30 min and rinsed with cold PBS, and the proteins were extracted as above. The neuronal survival was assayed using MTS (Promega) following the manufacturer's indications.

Statistical Analysis—Data were expressed as means ± S.D. The comparison between two mouse groups (WT and PS1×APP tg mice) was done by two-tailed *t* test. For comparison between several age groups, we used one-way analysis of variance followed by Tukey post hoc multiple comparisons test (Statgraphics plus 3.1). The significance was set at 95% of confidence.

RESULTS

Age-dependent Modifications on the GSK-3β Activity in PS1×APP Mouse Hippocampus—The GSK-3β activity could play a central role controlling apoptosis and the development of Alzheimer disease. Because GSK-3β activity was inhibited by phosphorylation on Ser-9, we have first quantified, by Western blots, the Ser-9 phospho-GSK-3β levels in our PS1×APP tg model. We used two different ages, 6 and 18 months, before and after pyramidal neurodegeneration, respectively (26, 30). Western blot analysis demonstrated the existence of a clear age-dependent variation of the Ser-9 phosphorylation levels in PS1×APP mice (Fig. 1*A*, *panels a1* and *a2*). As compared with 6-month-old WT mice, the levels of Ser-9 phospho-GSK-3β were elevated in young PS1×APP hippocampus, whereas the 18-month-old PS1×APP mice displayed a significant decrease. In fact, the Ser-9 phosphorylation level, at 18 months, represented a decrease of 5.66 ± 0.46 times over 6-month-old PS1×APP mice. This observation was also confirmed using immunohistochemistry. As shown in Fig. 1*B*, the phospho-Ser-9 GSK-3β immunoreactivity was mainly located in the somata of hippocampal neuronal cells. As also shown (Fig. 1*B*, *panels b1* and *b2*), a marked increase in the immunoreactivity was observed in the hippocampus of 6-month-old PS1×APP tg mice, as compared with WT. This increase was evident in both pyramidal and interneuronal cell somata and their proximal dendrites. In parallel experiments, GSK-3β phosphorylation immunostaining was clearly decreased in aged PS1×APP tg mice (Fig. 1*B*, *panels b3* and *b4*).

The GSK-3β activity could modulate the intrinsic apoptotic pathway by modifying, directly and/or indirectly, the expression of pro- and anti-apoptotic Bcl-2 family proteins (35–37). Thus, we have determined the possible variations in the expression of mRNAs coding for Bcl-2 proteins in 6- and 18-month-old WT and PS1×APP tg mice. According to the phosphorylation of the GSK-3β (38), in 6-month-old PS1×APP mice the expression of *bcl-2* was increased (Fig. 1*C*). On the contrary, in 18- month-old PS1×APP animals, the expression of *bcl-2* was not different from WT, whereas *bim* and *bad* expression increased exclusively in transgenic animals. These data could indirectly reflect the activation of GSK-3β in aged PS1×APP mice. Additionally, the possible age-dependent activation of the GSK-3β was also tested by determining the protein level and phosphorylation status of β-catenin (39). Although the phosphorylated *versus* total β-catenin ratio was not altered in 6-month-old PS1×APP mice (Fig. 1*D*), we did observed an increase in the steady-state levels of both β-catenin forms. These data were consistent with a reduced GSK-3β activity. More relevant and also consistent with the proposed age-dependent increase in the GSK-3β activity, the total and phosphorylated β-catenin contents were dramatically reduced in 18-month-old PS1×APP mice (Fig. 1*D*). Furthermore, the ratio of phospho/total β-catenin displayed a considerable increase in these aged PS1×APP mice, suggesting a hyperphosphorylation status of the β-catenin.

These data demonstrated the existence of an age-dependent change in the phosphorylation of the GSK-3β in our PS1×APP tg model. Whereas at early ages the GSK-3β seemed to be

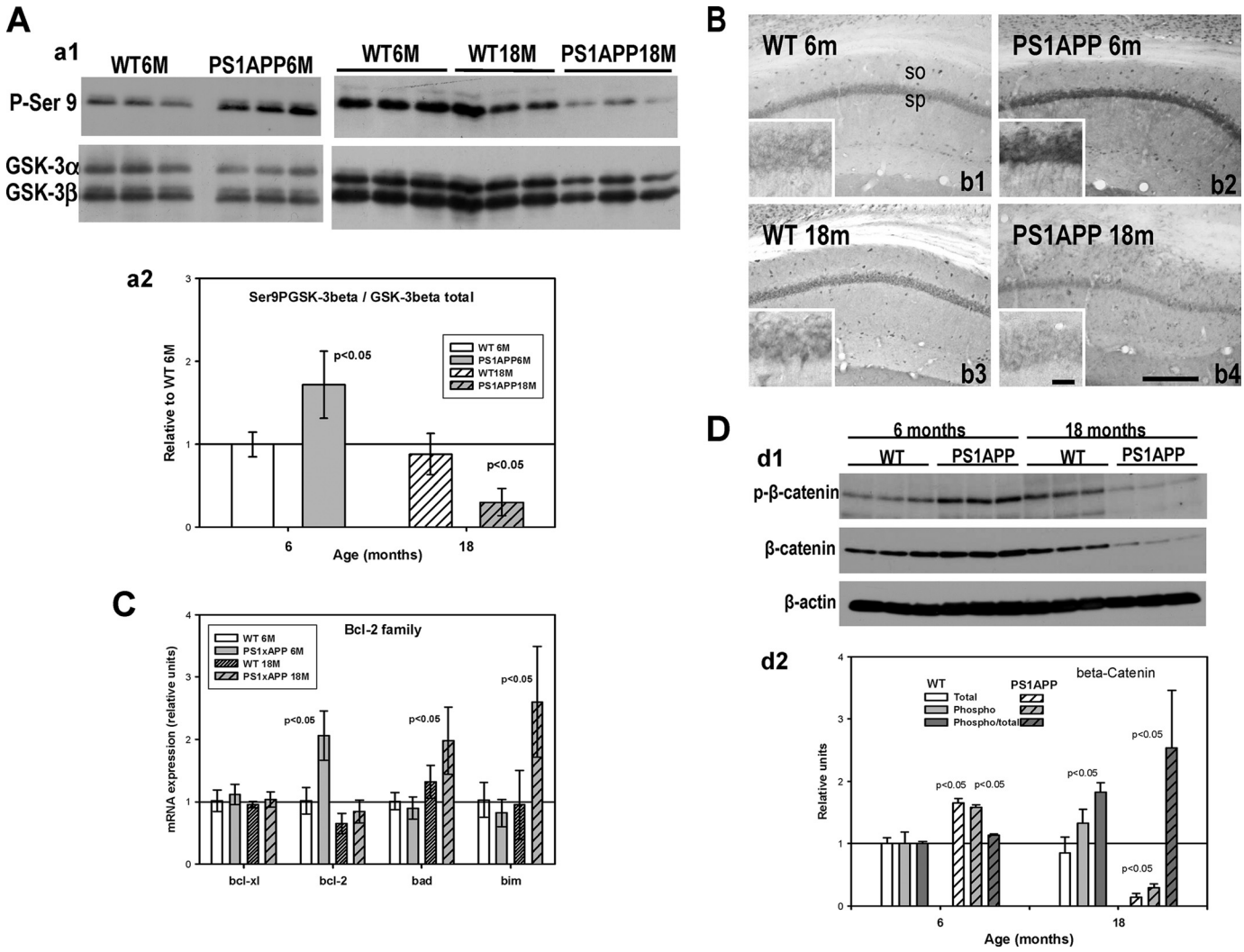

FIGURE 1. **Age-dependent decrease on GSK-3β phosphorylation (Ser-9) in PS1×APP hippocampus.** *A,* relative phosphorylation levels of Ser-9 GSK-3β (*panel a1, upper panel*) were determined, by Western blots, in 6- and 18-month-old WT and PS1×APP hippocampi. The Western blots were then reprobed for total GSK-3β (*a1, lower panel*). In these experiments, 10 μg of proteins from WT and PS1×APP mice were electrophoresed in parallel, using different distributions. In each gel, a minimum of three WT and three PS1×APP samples were run together. The experiment was repeated three times using different sample combinations. Quantitative analysis of the Western blots is shown in *panel a2*. The Western blots were scanned, and the ratio between phosphorylated/total expression was calculated. In each experiment, the phosphorylation/total ratio was normalized by 6-month-old WT value. The total protein loading was also tested by anti-β-actin antibody (data not shown). *B,* hippocampal (CA1) light microscopy images of phospho-Ser-9-GSK-3β immunohistochemistry from 6- (*panels b1* and *b2*) and 18-month-old (*panels b3* and *b4*) WT (*panels b1* and *b3*) and PS1×APP (*panels b2* and *b4*) mice. For these experiments, serial sections of 6- and 18 month-old WT and PS1×APP brains were processed in parallel. Thus, both WT and PS1×APP slices were equally developed. The image shown is representative of four different WT and PS1×APP mice. *Insets* show higher magnifications of stratum pyramidale. *C,* expression of different *bcl-2* family protein mRNAs was analyzed by quantitative RT-PCR. In each case, the results ($n = 7$) were corrected by the GAPDH expression and normalized by 6-month-old WT mice. *D,* total and phosphorylated β-catenin levels were assessed by Western blots (*panel d1*). Quantitative data are shown in *panel d2*. As shown, the total and phosphorylated β-catenin increased in samples from 6-month-old PS1×APP, and there was a dramatic decrease in both levels in samples from 18-month-old PS1×APP mice. Furthermore, the phosphorylated/total ratio also increased at this old age. Significance difference between the different samples was determined by analysis of variance followed by Tukey test. *so,* stratum oriens; *sp,* stratum pyramidale. *Scale bars,* 50 μm.

inhibited by Ser-9 phosphorylation (probably exerting a neuroprotective action), in aged PS1×APP mice the activation of GSK-3β was increased.

Young and Aged PS1×APP Hippocampus-derived Soluble Factors Increased or Inhibited, Respectively, the Akt-dependent Phosphorylation of GSK-3β—We next investigated the possibility that soluble APP-derived factors were involved in the modulation of GSK-3β phosphorylation in both young (6 months) and aged (18 months) PS1×APP mice. In this sense, it has been recently reported that monomeric Aβ42 mediated the activation of the PI3K-Akt pathway (40), whereas Aβ oligomers (ADDLs) induced an impairment of insulin receptors (27).

We have first determined *in vitro* using N2a cell cultures the effect of soluble brain extracts, derived from 6- and 18-month-old WT, PS1 (data not shown), and PS1×APP mice on the Ser-9 phosphorylation of GSK-3β. As shown (Fig. 2*A*, and quantitatively in Fig. 2*C*), the addition of the soluble fractions obtained from 6-month-old PS1×APP mice produced a clear induction in the GSK-3β phosphorylation over basal values (serum deprivation). This increase was mediated by the activation of the PI3K/Akt pathway because Akt was phosphorylated at both Thr-308 and Ser-473 residues (Fig. 2*A*), and the effect was abolished by the addition of LY294002 (data not shown). This activation of the PI3K/Akt pathway seemed to be mediated by at

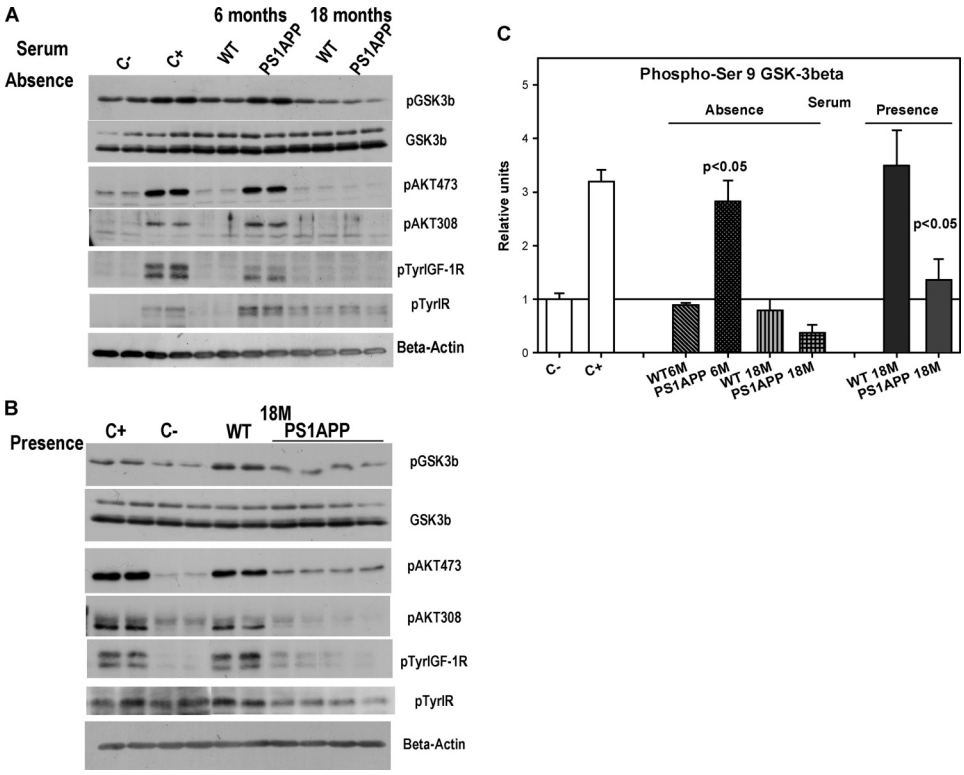

FIGURE 2. **Soluble fractions, derived from 6- or 18-month-old PS1×APP mice, produced the stimulation or inhibition of Akt-GSK-3β phosphorylation.** *A,* N2a cultures were serum-deprived for 12 h and treated with 50 μg of soluble proteins derived from young (6 months) or old (18 months) WT and PS1×APP mice. After treatment, the phosphorylation levels of GSK-3β (Ser-9), Akt (Ser-473 or Thr-308), IGF-1R (phospho-Tyr-1135/1136), or IR (phospho-Tyr-1150/1151) were determined by Western blots. As shown, the S1 fractions from 6-month-old PS1×APP produced a clear induction of the phosphorylation levels of all protein tested. *B,* possible inhibitory effect of 18-month-old PS1×APP S1 fractions (50 μg of protein) was assessed in serum-stimulated Akt-GSK-3β pathways. For each condition, two culture wells were treated in parallel, and the experiments were repeated at least three times. *C,* quantitative analysis of experiments shown in *A* and *B*. The results are mean ± S.D. of three independent experiments. Data were normalized by negative controls (*C*−). Negative (*C*−) and positive (*C*+) controls represented control experiments in the absence (12 h) or presence of serum, respectively. The protein loading was tested by total GSK-3 and β-actin.

least the IGF-1 and/or insulin receptors. In fact, both receptors were activated (Tyr-phosphorylated) in the presence of these soluble extracts. The activation of the Akt and phosphorylation of GSK-3β were specific for the factors present in PS1×APP mice because the addition of a similar amount of soluble proteins from WT or PS1 transgenic mice (data not shown) was devoid of any effect.

In parallel experiments, we have also tested the effect of soluble extracts from 18-month-old PS1×APP mice (Fig. 2, *A* and *C*). In contrast to that observed using young PS1×APP, 18-month-derived soluble fraction did not induce the phosphorylation of Akt-GSK-3β in serum-deprived cultures. In fact, a small inhibition, over control values, was observed (Fig. 2*C*). The soluble extracts from 18-month-old WT mice displayed no intrinsic effect.

The possible inhibitory action of the soluble fractions from aged transgenic mice was tested by analyzing their effect on the serum-stimulated Akt-GSK-3β phosphorylation. As shown (Fig. 2*B*), the treatment of N2a cells with fractions derived from 18-month-old PS1×APP mice produced a practically complete inhibition of the serum-induced GSK-3β phosphorylation (see also Fig. 2*C*). This inhibition was paralleled by a decrease in Akt473 and Akt308 phosphorylation and was also paralleled by a decrease in the Tyr phosphorylation of IGF-1R and insulin receptor. The soluble fractions from aged WT or PS1 (data not shown) mice showed no apparent effect.

In addition, we have also examined the effect of 6- and 18-month-derived soluble fractions on neuronal survival assays. For these experiments, primary neurons were subjected to deprivation and supplemented with 6- or 18-month soluble fractions. As expected (see supplemental Fig. 1), the soluble extract from 6-month-old PS1×APP avoided the decrease in neuronal survival due to growth factor deprivation. As also expected, the soluble fraction from 18 months did not protect or even produce a small decrease on the neuronal survival. In this sense, we also tested the possible neurotoxic effect of these 18-month PS1×APP-soluble fractions. After 24 h of incubation, in the presence of B27 supplement, these soluble fractions produced a significant decrease in the neuronal survival (100.0 ± 7.7% *versus* 80.19 ± 2.6%, $n = 3$; $p < 0.05$). The WT-derived soluble fractions displayed no intrinsic effect. These data demonstrated that soluble factors present exclusively in PS1×APP-derived brain fractions modulated (positively or negatively) the GSK-3β phosphorylation and neuronal survival.

Characterization of APP-derived Fragments from Young and Aged PS1×APP Mice—As mentioned above, APP-derived proteins could modulate the GSK-3β phosphorylation. In consequence, we have next analyzed, by Western blots using the mAb 6E10 (Fig. 3*A*), the presence of APP-derived soluble fragments in these fractions. As shown, the soluble fractions from 6-month-old PS1×APP mice exhibited a single specific (as compared with WT) band of high apparent molecular weight

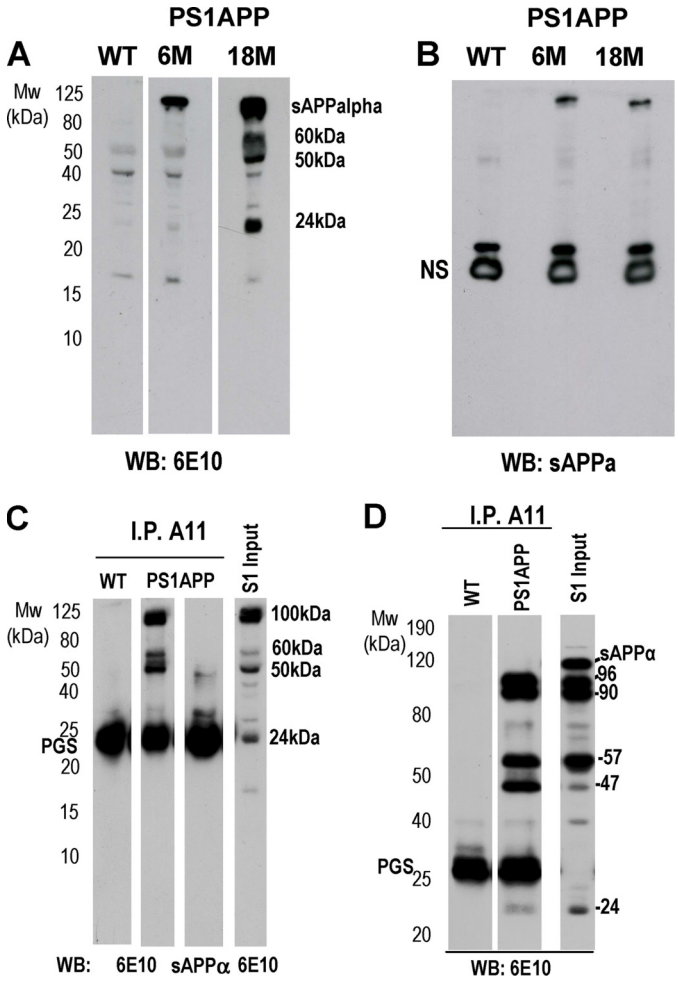

FIGURE 3. **Aβ oligomeric forms in soluble extracts from 18-month PS1×APP.** *A,* S1 fractions from 6 month-old WT and PS1×APP or 18-month PS1×APP were first analyzed by Western blot (16% SDS-Tris-Tricine-PAGE) using mAb 6E10. Results showed an age-dependent increase of soluble SDS-resistant oligomeric species of approximately 24, 50, 60, and 90 kDa in PS1×APP animals. No significant amounts of mono-, di-, or trimers were detected under these experimental conditions. *B,* Western blots (*WB*) were re-tested using anti-sAPPα antibody. Only a high molecular weight specific band (~90 kDa) was observed. No significant (*NS*) age-dependent changes could be appreciated in this band. *C,* immunoprecipitation (*I.P.*) experiments using A11 antibody were addressed for selective recognition of the Aβ oligomers in 18-month PS1×APP-soluble extracts. The S1 fractions obtained from 18-month-old WT or PS1×APP were incubated with A11-protein G-Sepharose immunocomplexes and analyzed by 16% SDS-Tris-Tricine-PAGE and Western blots using 6E10. As shown, the pattern of immunoisolated Aβ oligomers was similar to that observed in the crude S1 fraction. Anti-sAPPα antibody displayed no specific staining in these immunoprecipitated samples. *D,* A11 immunoisolated oligomers were resolved using 12%-SDS-Tris glycine-PAGE and blotted as in *C*. Using this approach, at least five different Aβ oligomeric forms were identified. Western blots are representative of at least four replicated experiments with similar results.

(Fig. 3*A*). Interestingly, no monomeric Aβ was detected by this assay, even after longer exposures (data not shown). Because mAb 6E10 recognized both Aβ peptides and sAPPα, we retested the Western blots using an anti-sAPPα antibody. As shown (Fig. 3*B*), a band of similar relative molecular weight (M_r) was also observed with this antibody. Therefore, sAPPα was the predominant APP-derived fragment (detected with 6E10) in young PS1×APP mouse hippocampi.

However, the analysis of the soluble fractions from 18-month-old PS1×APP mouse hippocampi demonstrated the presence of several oligomeric Aβ forms. Based on the calculated M_r (24, 50, and 60–70 kDa), these Aβ oligomers were compatible with the presence of 6- and 12–16-mer, SDS-resistant aggregates. As expected, these oligomers were immunopositive for A11 and Nu-1 antibodies in dot blots (data not shown but see Ref. 26). It is also interesting the absence of monomeric Aβ in these fractions. It is of note that the presence of a relatively abundant band localized in the high molecular weight range. This band probably corresponded to a different highly aggregated Aβ oligomer because, as probed by Western blots using anti-sAPPα antibody, this soluble fragment did not increase in aged PS1×APP mice (see Fig. 2*B*).

To further characterize these Aβ oligomers, we used the conformation-dependent anti-oligomeric A11 antibody in immunoprecipitation assays. As shown (Fig. 3*C*), three different high molecular weight Aβ oligomers (50, 60–70, and 90–100 kDa) were immunoprecipitated by A11 antibody. The 24-kDa oligomer was occluded by the presence of a prominent band corresponding to the protein G-Sepharose. This putative 6-mer oligomer was clearly visualized using A11-protein A-Sepharose immunocomplexes (data not shown but see below). Furthermore, as expected, A11 antibody did not immunoprecipitate the sAPPα (Fig. 3*C*).

To better resolve these relatively high molecular weight Aβ oligomers, the A11-immunoprecipitated proteins were also analyzed in 12% Tris glycine gels (Fig. 3*D*). As shown, at least five different putative Aβ oligomers (detected by 6E10) of 24, 47, 57, 90, and 96 kDa were identified in these experiments. As also shown, the sAPPα (110-kDa band), present in the soluble fraction, was not immunoprecipitated by A11. Therefore, the aggregated forms presented in the soluble fractions from 18-month-old PS1×APP mice were compatible with the presence of Aβ oligomers of 6-, 10-, 12-, 20- and 22-mers.

Opposite Actions of Synthetic sAPPα (Stimulation) and ADDLs (Inhibition) on the Akt Prosurvival Pathway—Based on the observed soluble fraction composition, we next characterized the effect of synthetic sAPPα and Aβ oligomers on the Akt-GSK-3β phosphorylation (Fig. 4) using N2a cell cultures.

The soluble APPα (Fig. 4*A*, *panel a1,* and quantitatively in *panel a2*) produced a dose-dependent increase in the phosphorylation levels of Ser-9 GSK-3β and Akt (at Thr-308 and Ser-473 residues), whereas the soluble APPβ, probed in parallel experiments, produced no effect in this *in vitro* phosphorylation assay (Fig. 4*A*, *panel a2*). Interestingly, the sAPPα displayed a quite high potency in the low nanomolar range (EC_{50} = 2.30 ± 0.93 nM, n = 4; Fig. 4*A*, *panel a2*) coincident with the estimated concentration (by Western blots using commercial sAPPα as standard) of the sAPPα in the soluble fraction of the 6-month-old PS1×APP mice (19.9 ± 4.11 nM). This stimulatory effect was also replicated using primary cortical cultures (supplemental Fig. 3*A*). As expected, sAPPα seemed to exert its effect acting through IGF-1R and insulin receptor (see Fig. 4*A*, *panel a1*) and, in consequence, was inhibited by LY294002, AG1024, and picropodophyllin (supplemental Fig. 2*A*).

These data indicated that in this *in vitro* model the sAPPα behaved like an agonist, acting at least through IGF-1R and insulin receptors, activating the PI3K/Akt pathway and, in consequence, phosphorylating and inhibiting the GSK-3β activity.

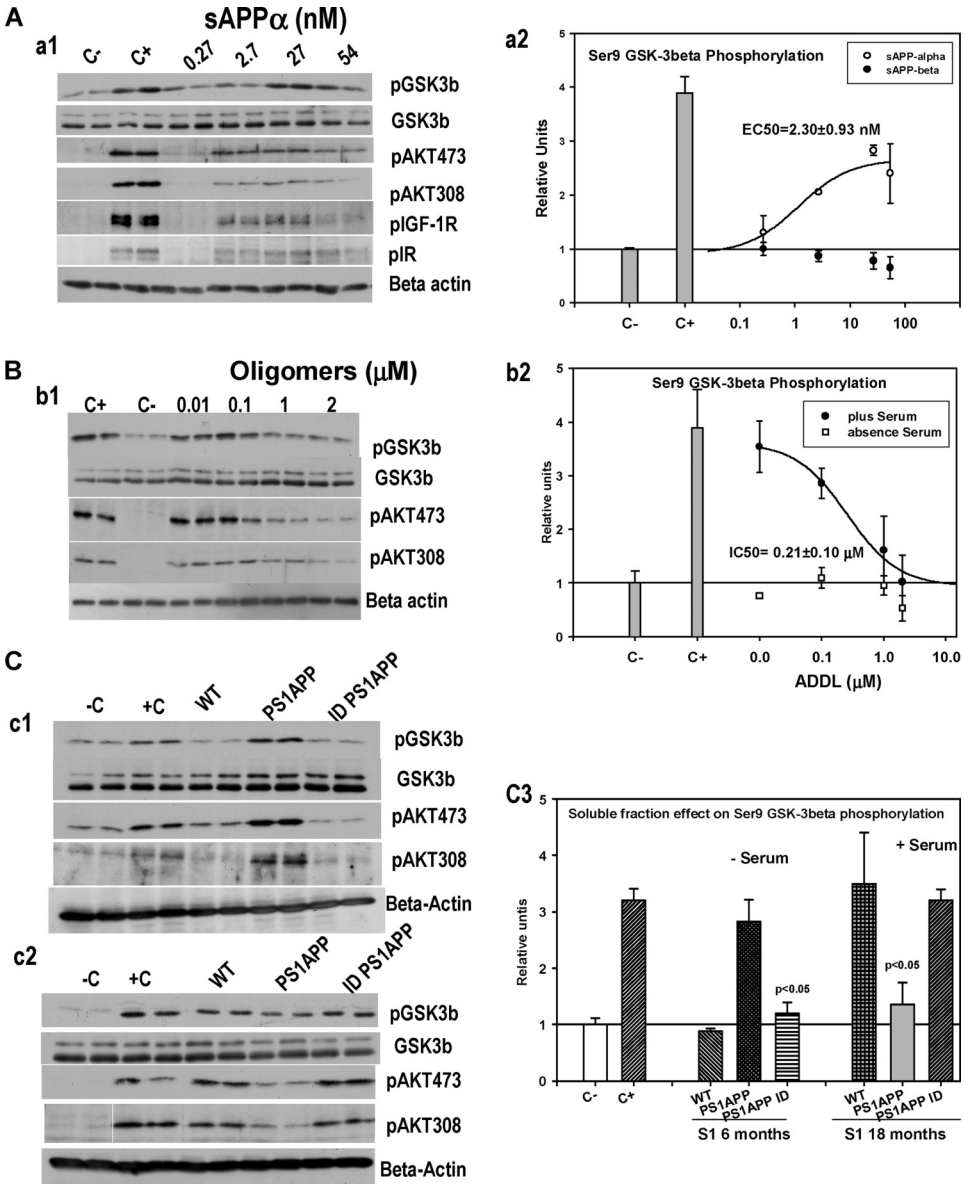

FIGURE 4. **Synthetic sAPPα and Aβ oligomers (ADDLs) stimulated or inhibited the Akt-GSK-3β phosphorylation in N2a cultures.** *A,* sAPPα activated the IGF-1R/IR Akt GSK-3β pathway. Serum-deprived N2a cultures were treated with increasing concentrations of synthetic sAPPα or sAPPβ (data not shown), and the phosphorylations of Ser-9 GSK-3β, Akt (473 and 308), IGF-1R (Tyr-1135/1136), and IR (Tyr-1150/1151) were analyzed by Western blots (*panel a1*). *Panel a2,* quantitative analysis of Western blots normalized by negative control (*C*−). *B,* inhibitory effect of increased concentrations of ADDLs on Akt-GSK-3β phosphorylation was assessed in N2a maintained in the presence of serum. Western blots (*panel b1*) and quantitative analysis of the data (*panel b2*) are illustrated. *C,* immunodepletion experiments. The S1 fractions, derived from 6- (*panel c1*) or 18-month-old (*panel c2*) PS1×APP mice, were immunodepleted using 6E10 or A11, and the samples were tested for stimulation experiments (as above) in the absence (*panel c1*) or presence of serum (*panel c2*). *Panel c3,* quantitative analysis of the Western blots. Data were normalized by the corresponding negative control and are means ± S.D. of three independent experiments. Data (mean ± S.D.) presented in *panels a2* and *b2* were fitted to a logistic four-parameter equation as described previously (34, 62). The protein loading was tested by total GSK-3β and β-actin.

In addition, saturating concentrations of sAPPα promoted neuronal survival in a deprivation assay (supplemental Fig. 2*B*).

Aiming to test the possible inhibitory effect of oligomeric Aβ, we have used synthetic Aβ oligomers (ADDLs) (41). Similar to natural Aβ oligomers, the synthetic ADDLs displayed no intrinsic effect in the absence of serum (data not shown). Also similar to natural oligomers, in the presence of serum, ADDLs displayed a dose-dependent inhibition of the GSK-3β phosphorylation (Fig. 4*B*, *panel b1*) with a calculated IC_{50} of 0.21 ± 0.10 μM ($n = 4$) (Fig. 4*B*, *panel b2*). As expected from our previous data, this inhibitory effect was paralleled by an inhibition of the serum-stimulated Akt activation (pAkt473 and -308) (Fig. 4*B*, *panel b1*). This inhibitory effect was also replicated in primary neuronal cultures (supplemental Fig. 3*B*).

In addition, we have tested the possible neuroprotective effect of sAPPα and 6-month PS1×APP-soluble fractions on ADDL (2 μM) toxicity (supplemental Fig. 3*C*). As shown, the sAPPα and 6-month PS1×APP soluble fractions avoided (partially and fully, respectively) the ADDL-induced neuronal toxicity.

Based on these observations, we postulated that if the stimulation (at 6 months) or inhibition (18 months) of the Akt-

GSK-3β phosphorylation was indeed mediated by sAPPα, at 6 months, or Aβ oligomers, at 18 months, their effect should be avoided by immunodepletion using 6E10 (for sAPPα) or A11 (for Aβ oligomers). Therefore, we tested the stimulation or inhibition of Akt-GSK-3β phosphorylation after three sequential immunodepletions of the soluble fractions with either 6E10 (for 6 months) or A11 (18 months). The results are shown in Fig. 4*C* (and quantitatively in Fig. 4*C*, *panel c3*). As expected, after immunodepletion with 6E10, the stimulatory action of the 6-month-derived fractions was completely avoided (Fig. 4*C*, *panel c1*). Neither GSK-3β nor Akt 473/308 was phosphorylated after 6E10 immunodepletion. Conversely, the inhibitory effect of the 18-month-derived fraction was completely reversed by A11 immunodepletion (Fig. 4*C*, *panel c2*). As shown, the serum-induced GSK-3β and Akt473/308 phosphorylation was almost completely re-established after A11 treatment.

Therefore, at young ages in our PS1×APP model, the production of sAPPα determined the activation of Akt and the phosphorylation of Ser-9-GSK-3β (throughout at least IGF-1 and/or insulin receptors), whereas the age-dependent appearance of soluble oligomeric forms of Aβ determined the inhibition of this pro-survival pathway.

Synthetic Aβ Oligomers Inhibit the Activation of Prosurvival Receptors—Because of the relevance of the inhibition of the pro-survival pathways in the development of AD, we have further evaluated the inhibitory properties of the oligomeric Aβ using *in vitro* assays. It has been suggested that Aβ oligomers could inhibit the prosurvival Akt-GSK-3β phosphorylation by direct interaction with at least insulin receptors (42) and/or produced insulin resistance (27, 43). To ascertain the possible specificity in the ADDL inhibition, we determined the effect of two different concentrations of ADDLs (0.2 and 2 μM) on the stimulatory effect of IGF-1, insulin, BDNF, NGF, and sAPPα (Fig. 5*A*, *panels a1* and *a2*). As expected, the addition of the different factors produced the phosphorylation of the GSK-3β, demonstrating the presence of functional receptors in the N2a cells. As also shown in Fig. 5*A*, ADDLs inhibited the induced GSK-3β phosphorylation for all factors tested. Importantly, the effect of ADDLs displayed a clear selectivity on the inhibitory action. As shown, the NGF stimulation of GSK-3β phosphorylation seemed to be preferentially inhibited. In fact, 0.2 μM ADDLs completely blocked the NGF stimulation. In contrast, BDNF stimulation displayed low sensitivity to the ADDL effect. Only a minor inhibition could be observed at the highest dose used (2 μM). Insulin, IGF-1. and sAPPα presented intermediated sensitivity.

This selectivity could indicate that ADDLs might interact directly with the different trophic receptors. Theoretically, if both ligands exert their action through the same receptor, the ADDL inhibition should be reverted by increasing the trophic factor concentration. In fact, the inhibitory effect of submaximal doses of ADDLs (20 nM) was totally reverted by increasing concentrations of NGF (Fig. 5*B*, *panels b2* and *b2*). Similar results were observed using IGF-1 or insulin (data not shown). Based on these data, we cannot discriminate between a direct inhibition or a negative allosteric effect of ADDLs. However, these data indicated that the inhibitory action of Aβ oligomers was, at least in part, mediated by a direct interaction with different prosurvival receptors. In fact, ADDLs inhibited the Tyr phosphorylation of IGF-1, insulin, and Trk-A receptors (supplemental Fig. 4). The results indicated that for all three receptors the addition of ADDLs prevented the Tyr phosphorylation and, consequently, the receptor activation. This effect was particularly evident for IGF-1R. Therefore, the ADDLs seemed to be acting primordially at the activation level of the different receptors tested.

DISCUSSION

Multiple APP-based transgenic mouse models have been developed to evaluate the neurological deficiencies observed in AD. However, none of them displayed all pathological signs of the disease. The most relevant discrepancies between AD and the transgenic models were the absence of Tau phosphorylation and late, if any, neuronal degeneration, even in the presence of large Aβ accumulation since early ages. This apparent age-dependent neuroprotective/neurodegenerative status has not yet been fully addressed. Here, using *in vivo* and *in vitro* assays, we demonstrated the following. 1) sAPPα acting through IGF-1R and insulin receptors activated the prosurvival PI3K-Akt-GSK-3β pathway, which might explain the lack of neuronal death in most transgenic models at early/middle ages. 2) The age-dependent increase in soluble Aβ oligomers blocked the neurotrophin (including sAPPα)-mediated prosurvival pathway, explaining the observed late neuronal vulnerability.

It has been postulated that GSK-3β activity might exert a central role in the development of AD. GSK-3β activity was implicated in Tau phosphorylation, APP processing, Aβ production, and neurodegeneration (15). Overexpression of GSK-3β in a conditional transgenic model produced Tau hyperphosphorylation and neuronal death (16, 44). Furthermore, pharmacological inhibition of the GSK-3β activity by lithium decreased Aβ production and plaque accumulation (45), improved performance in memory tests, preserved the dendritic structure, and reduced the Tau-dependent pathology in AD tg models (46, 47).

Therefore, in this study we have first determined the Ser-9 phosphorylation levels in young/middle (6 months) and aged (18 months) PS1×APP mice, before and after pyramidal cell neurodegeneration in hippocampus, respectively (26). Accordingly, with a putative neuroprotective environment at early/middle ages, young PS1×APP mice displayed significantly higher levels of neuronal GSK-3β Ser-9 phosphorylation, suggesting a decreased activity of this enzyme. Also, we have observed an increased expression of the anti-apoptotic Bcl-2 protein (38) and the increase in the β-catenin protein. These data could indicate the presence of increased levels of neurotrophins in this tg model. However, except for IGF-1, which was locally increased around the Aβ plaques (although its total concentration decreased in 6- and 18-month PS1×APP mice, results not shown), none of the growth factors analyzed were modified in our transgenic model (data not shown). On the contrary, we demonstrated that soluble fractions derived from 6-month-old PS1×APP, and not from WT or PS1, activated the IGF-1R/IR-Akt pathway, phosphorylated the GSK-3β, and in

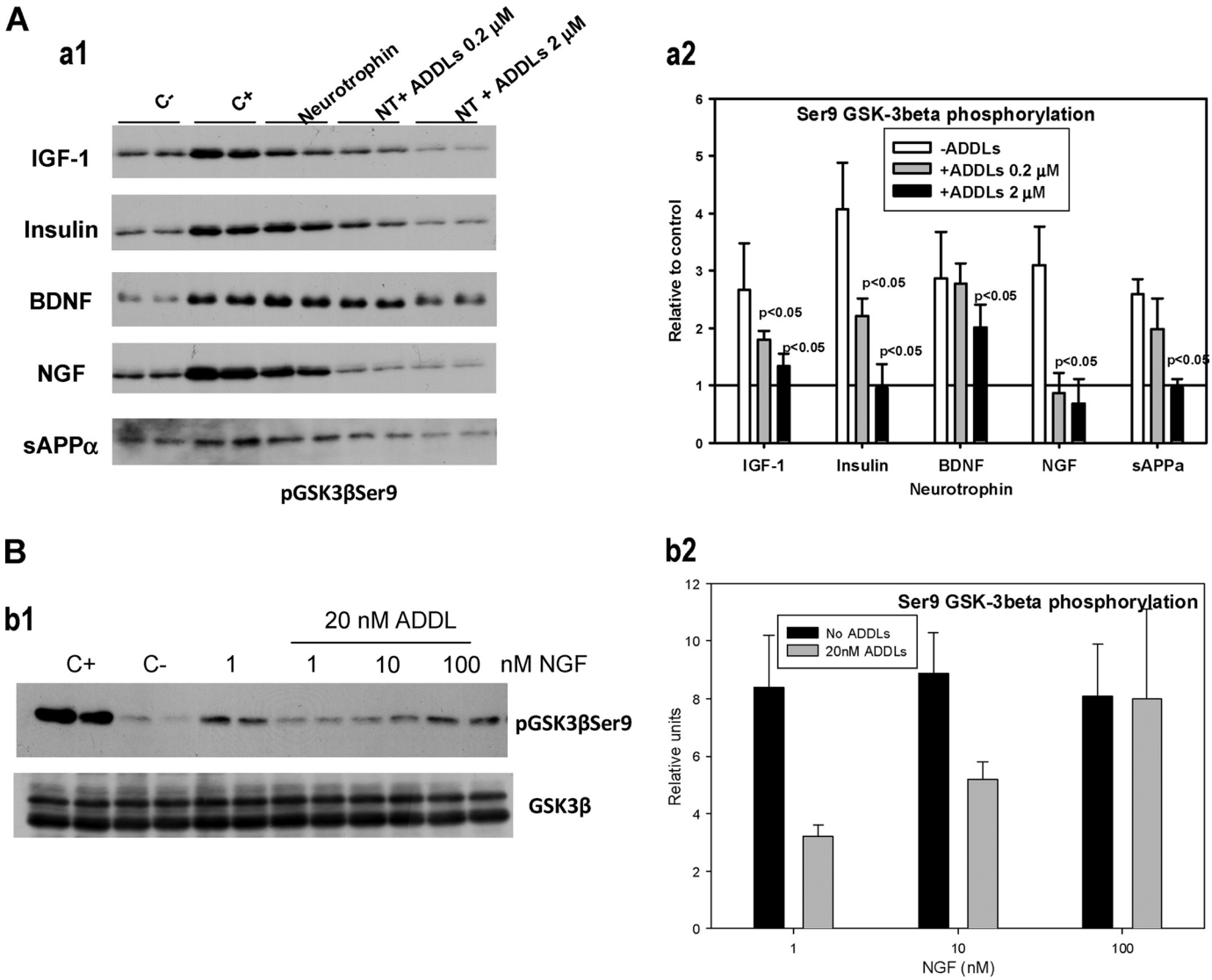

FIGURE 5. **Synthetic Aβ oligomers (ADDLs) competed with different neurotrophins for the stimulation of Ser-9 GSK-3β phosphorylation.** *A,* for competition experiments, the Ser-9 GSK-3β phosphorylation was stimulated by a fixed concentration of different neurotrophins and 0.2 or 2 μM ADDLs. After treatment, the Ser-9 GSK-3β phosphorylation was determined by Western blots (*panel a1*) and quantitatively (*panel a2*) after normalization by negative controls. *B,* inhibitory effect of ADDLs, at submaximal doses (20 nM) was reverted by increasing the concentration of different neurotrophins, such as NGF, IGF-1 or insulin. In these experiments, N2a cells were treated with different concentrations of each neurotrophin in the absence (data not shown) or presence (*panel b1*) of ADDLs. After Western blots, the GSK-3β phosphorylation was quantitatively analyzed (*panel b2*) and normalized by negative controls. *C*−, negative control; *C*+, positive control.

consequence, promoted the neuronal survival in primary cultures.

Within the different APP-derived fragments, both soluble APPα and -β (data not shown) were the predominant APP peptides identified in the tg-soluble fractions. Although the monomeric Aβ could also produce a similar effect (data not shown) (40), no significant amounts of monomeric Aβ were detected in 6-month-derived soluble extracts.

The implication of sAPPα in the activation of the Akt prosurvival pathway was further demonstrated *in vitro*, using synthetic sAPPα. The sAPPα produced a dose-dependent activation of the Akt-GSK-3β pathway that was inhibited by LY294002, AG1024, and picropodophyllin and mediated by the activation of, in this *in vitro* assay, IGF-1 and insulin receptors. Moreover, the effect of 6-month-old PS1×APP brain-derived fractions was completely avoided by immunodepletion experiments using 6E10. Furthermore, the estimated sAPPα concentration in the soluble fractions (~20 nM) was in the range of the calculated EC_{50} for synthetic sAPPα (2.3 nM). Interestingly, the sAPPβ fragment displayed no intrinsic activity in this *in vitro* model. To the best of our knowledge, this is the first time that the effect of sAPPα on Akt-GSK-3β pathway has been directly demonstrated.

The present data cannot demonstrate, *in vivo*, a direct cause-effect relationship between the presence of sAPPα and GSK-3β phosphorylation. However, we might postulate that, in our model, the overexpression of the tg APP produced increased amounts of sAPPα and, because of its agonist-like effect on the prosurvival receptors, could to some extent delay the Aβ pathology. In fact, although the increase in GSK-3β phosphorylation was not observed in all APP-based tg models (48, 49), all models exhibited a considerable delay between the Aβ deposi-

tion and the appearance of neuronal pathology (if any). Thus, data presented in this work add a new connection between APP metabolism and GSK-3β regulation that could explain the slow pathological progression, observed in all transgenic models, and also the decrease in tauopathy[6] and increased survival of some bigenic APP-Tau models (50). Moreover, the activation of the α-secretase activity, with a parallel increase in sAPPα secretion, could constitute a novel therapeutic approach in AD (51).

In addition, we have also demonstrated the inhibitory effect of natural oligomeric forms of Aβ on the Akt-GSK-3β pathway. It should be noted the presence of five different soluble, SDS-resistant Aβ oligomers of 24, 47, 57, 90, and 96 kDa in the 18-month PS1×APP brain-derived fractions. The identity of these Aβ oligomeric peptides was confirmed using the polyclonal anti-oligomeric antibody A11 in immunoprecipitation experiments, followed by Western blots using 6E10. These results confirmed our previous data using this tg model (26 and also see Refs. 20, 23).

We observed a clear inhibition of Akt phosphorylation when N2a cells were treated with soluble fractions derived from 18-month-old PS1×APP tg mice (see also Ref. 52). This inhibition seemed to be mediated by a direct effect on trophic receptors because activation (Tyr phosphorylation) of at least IGF-1 and insulin receptors was inhibited by the addition of these soluble fractions. Furthermore, this inhibitory effect was exclusively due to the presence of Aβ oligomers, because the immunodepletion of Aβ oligomers, using A11, completely reversed the inhibitory effect. Thus, the age-dependent appearance of extracellular Aβ oligomers could inhibit the Akt-GSK-3β pro-survival pathway. This inhibitory effect was consistent with the age-dependent decrease in the Ser-9-GSK-3β phosphorylation, the increase in phosphorylated Tau (results not shown), and the β-catenin hyperphosphorylation and degradation observed in hippocampal samples from 18-month-old PS1×APP mice. In addition, as we recently reported, the presence of extracellular Aβ oligomers determined the potential cytotoxic microglial activation, coincidentally with CA1 pyramidal cell loss (26). Those data, together with the present observations, demonstrated that accumulation of extracellular Aβ oligomers determined the inhibition of the prosurvival pathways coincidentally with the activation of a potentially cytotoxic inflammatory response. Both actions could indeed create the appropriate environment to induce the observed neuronal death.

Our data also indicated that ADDLs could exert their inhibitory action by a direct effect on the different trophic receptors. This assessment was based on the following: (i) the higher ADDL selectivity for NGF than for BDNF, and (ii) the reversion of the inhibitory effect by increasing concentrations of the neurotrophin (NGF, insulin, or IGF-1). A possible direct effect of Aβ oligomers and IR has been also suggested previously (27, 42). However, we cannot discard that ADDLs might also exert an inhibitory action by a different mechanism. In this sense, it has been suggested that ADDLs, acting on other different receptors such as *N*-methyl-D-aspartic acid or p75NTR (53–55), could reduce or even inhibit the insulin response (27, 43) through Akt473 phosphorylation with no activation of the pathway. However, in our *in vitro* system, the phosphorylation of Akt473 always paralleled Akt308 and GSK-3β Ser-9, even using primary neuronal cultures (data not shown). We do not know the origin of this disagreement; however, in our *in vitro* assays, the cells were incubated with ADDLs for a short time (20–30 min) in order to minimize the possible cellular death. Thus, it is possible that longer ADDL treatment was required.

Concerning the possible physiological relevance of our observations, it should be mentioned that chronic decrease in the trophic signaling, such as NGF, could be implicated in AD development (7, 56, 57). In this sense, the selective inhibitory effect of Aβ oligomers (NGF > IGF-1 = insulin > BDNF) might contribute to this decreased signal and, in consequence, be implicated in the preferential vulnerability of the cholinergic system observed in AD. It has also been demonstrated that Aβ oligomers could directly bind to p75NTR (55, 58) producing the formation of neuritic dystrophies (also observed in our model) (30, 59, 60) and the activation of c-Jun kinases mediating cell degeneration (61). Thus, the appearance of Aβ oligomers could actively decrease the trophic support, interacting with trophic receptors (this work), and/or increase the toxic signaling activating death receptors such as p75NTR.

In summary, our data demonstrated that the presence of soluble factors in PS1×APP mice modulated the GSK-3β Ser-9 phosphorylation. In young tg mice, sAPPα, acting at least through IGF-1R and IR, determined the activation of Akt-GSK-3β phosphorylation pathway. The activation of this pathway, classically assigned as pro-survival, could influence the limited Tau phosphorylation and neuronal degeneration observed in most tg models. At relatively late ages (18 months), the presence of multiple Aβ oligomeric forms determined the inhibition of the signal of all neurotrophins tested. The effect of Aβ oligomers might be mediated by interaction with the different receptors, although a different and more complex action cannot be discarded. This *in vitro* inhibition of the prosurvival signal was also supported with *in vivo* data, demonstrating a decrease in GSK-3β Ser-9 phosphorylation and an increase in AT100 immunoreactivity. Revealing the prosurvival pathways used by the different vulnerable neuronal subsets will provide further insights into the molecular mechanisms of AD pathogenesis.

Acknowledgments—We thank Drs. W. Klein and M. Lambert for their generous gift of Nu-1 antibody and Dr. I Torres-Aleman for IGF-1 determination.

[6] J. Vitorica, unpublished results.

REFERENCES

1. Haass, C., and Selkoe, D. J. (2007) *Nat. Rev. Mol. Cell Biol.* **8,** 101–112
2. Thoenen, H. (1995) *Science* **270,** 593–598
3. Tropea, D., Kreiman, G., Lyckman, A., Mukherjee, S., Yu, H., Horng, S., and Sur, M. (2006) *Nat. Neurosci.* **9,** 660–668
4. Ernfors, P., and Bramham, C. R. (2003) *Trends Neurosci.* **26,** 171–173
5. Schulte-Herbrüggen, O., Jockers-Scherübl, M. C., and Hellweg, R. (2008) *Curr. Alzheimer Res.* **5,** 38–44
6. Mufson, E. J., Counts, S. E., Perez, S. E., and Ginsberg, S. D. (2008) *Expert Rev. Neurother.* **8,** 1703–1718
7. Capsoni, S., Tiveron, C., Vignone, D., Amato, G., and Cattaneo, A. (2010) *Proc. Natl. Acad. Sci. U.S.A.* **107,** 12299–12304

8. Cole, G. M., and Frautschy, S. A. (2007) *Exp. Gerontol.* **42,** 10–21
9. Moloney, A. M., Griffin, R. J., Timmons, S., O'Connor, R., Ravid, R., and O'Neill, C. (2010) *Neurobiol. Aging* **31,** 224–243
10. Hoyer, S. (1998) *J. Neural Transm.* **54,** 187–194
11. Steen, E., Terry, B. M., Rivera, E. J., Cannon, J. L., Neely, T. R., Tavares, R., Xu, X. J., Wands, J. R., and de la Monte, S. M. (2005) *J. Alzheimer Dis.* **7,** 63–80
12. Reger, M. A., Watson, G. S., Green, P. S., Wilkinson, C. W., Baker, L. D., Cholerton, B., Fishel, M. A., Plymate, S. R., Breitner, J. C., DeGroodt, W., Mehta, P., and Craft, S. (2008) *Neurology* **70,** 440–448
13. Carro, E., Trejo, J. L., Gomez-Isla, T., LeRoith, D., and Torres-Aleman, I. (2002) *Nat. Med.* **8,** 1390–1397
14. Bondy, C. A., and Cheng, C. M. (2004) *Eur. J. Pharmacol.* **490,** 25–31
15. Balaraman, Y., Limaye, A. R., Levey, A. I., and Srinivasan, S. (2006) *Cell. Mol. Life Sci.* **63,** 1226–1235
16. Lucas, J. J., Hernández, F., Gómez-Ramos, P., Morán, M. A., Hen, R., and Avila, J. (2001) *EMBO J.* **20,** 27–39
17. Peineau, S., Taghibiglou, C., Bradley, C., Wong, T. P., Liu, L., Lu, J., Lo, E., Wu, D., Saule, E., Bouschet, T., Matthews, P., Isaac, J. T., Bortolotto, Z. A., Wang, Y. T., and Collingridge, G. L. (2007) *Neuron* **53,** 703–717
18. Woodgett, J. R., and Ohashi, P. S. (2005) *Nat. Immunol.* **6,** 751–752
19. Beurel, E., and Jope, R. S. (2006) *Prog. Neurobiol.* **79,** 173–189
20. Gong, Y., Chang, L., Viola, K. L., Lacor, P. N., Lambert, M. P., Finch, C. E., Krafft, G. A., and Klein, W. L. (2003) *Proc. Natl. Acad. Sci. U.S.A.* **100,** 10417–10422
21. Lacor, P. N., Buniel, M. C., Chang, L., Fernandez, S. J., Gong, Y., Viola, K. L., Lambert, M. P., Velasco, P. T., Bigio, E. H., Finch, C. E., Krafft, G. A., and Klein, W. L. (2004) *J. Neurosci.* **24,** 10191–10200
22. De Felice, F. G., Wu, D., Lambert, M. P., Fernandez, S. J., Velasco, P. T., Lacor, P. N., Bigio, E. H., Jerecic, J., Acton, P. J., Shughrue, P. J., Chen-Dodson, E., Kinney, G. G., and Klein, W. L. (2008) *Neurobiol. Aging* **29,** 1334–1347
23. Lesné, S., Koh, M. T., Kotilinek, L., Kayed, R., Glabe, C. G., Yang, A., Gallagher, M., and Ashe, K. H. (2006) *Nature* **440,** 352–357
24. Shankar, G. M., Bloodgood, B. L., Townsend, M., Walsh, D. M., Selkoe, D. J., and Sabatini, B. L. (2007) *J. Neurosci.* **27,** 2866–2875 .
25. Deshpande, A., Mina, E., Glabe, C., and Busciglio, J. (2006) *J. Neurosci.* **26,** 6011–6018
26. Jimenez, S., Baglietto-Vargas, D., Caballero, C., Moreno-Gonzalez, I., Torres, M., Sanchez-Varo, R., Ruano, D., Vizuete, M., Gutierrez, A., and Vitorica, J. (2008) *J. Neurosci.* **28,** 11650–11661
27. Zhao, W. Q., De Felice, F. G., Fernandez, S., Chen, H., Lambert, M. P., Quon, M. J., Krafft, G. A., and Klein, W. L. (2008) *FASEB J.* **22,** 246–260
28. Griffin, R. J., Moloney, A., Kelliher, M., Johnston, J. A., Ravid, R., Dockery, P., O'Connor, R., and O'Neill, C. (2005) *J. Neurochem.* **93,** 105–117
29. Blanchard, V., Moussaoui, S., Czech, C., Touchet, N., Bonici, B., Planche, M., Canton, T., Jedidi, I., Gohin, M., Wirths, O., Bayer, T. A., Langui, D., Duyckaerts, C., Tremp, G., and Pradier, L. (2003) *Exp. Neurol.* **184,** 247–263
30. Ramos, B., Baglietto-Vargas, D., del Rio, J. C., Moreno-Gonzalez, I., Santa-Maria, C., Jimenez, S., Caballero, C., Lopez-Tellez, J. F., Khan, Z. U., Ruano, D., Gutierrez, A., and Vitorica, J. (2006) *Neurobiol. Aging* **27,** 1658–1672
31. Caballero, C., Jimenez, S., Moreno-Gonzalez, I., Baglietto-Vargas, D., Sanchez-Varo, R., Gavilan, M. P., Ramos, B., Del Rio, J. C., Vizuete, M., Gutierrez, A., Ruano, D., and Vitorica, J. (2007) *J. Neurosci. Res.* **85,** 787–797
32. Lambert, M. P., Velasco, P. T., Chang, L., Viola, K. L., Fernandez, S., Lacor, P. N., Khuon, D., Gong, Y., Bigio, E. H., Shaw, P., De Felice, F. G., Krafft, G. A., and Klein, W. L. (2007) *J. Neurochem.* **100,** 23–35
33. Kayed, R., Head, E., Thompson, J. L., McIntire, T. M., Milton, S. C., Cotman, C. W., and Glabe, C. G. (2003) *Science* **300,** 486–489
34. Araujo, F., Tan, S., Ruano, D., Schoemaker, H., Benavides, J., and Vitorica, J. (1996) *J. Biol. Chem.* **271,** 27902–27911
35. Scali, C., Caraci, F., Gianfriddo, M., Diodato, E., Roncarati, R., Pollio, G., Gaviraghi, G., Copani, A., Nicoletti, F., Terstappen, G. C., and Caricasole, A. (2006) *Neurobiol. Dis.* **24,** 254–265
36. Hongisto, V., Smeds, N., Brecht, S., Herdegen, T., Courtney, M. J., and Coffey, E. T. (2003) *Mol. Cell. Biol.* **23,** 6027–6036
37. Lonze, B. E., and Ginty, D. D. (2002) *Neuron* **35,** 605–623
38. Karlnoski, R., Wilcock, D., Dickey, C., Ronan, V., Gordon, M. N., Zhang, W., Morgan, D., and Taglialatela, G. (2007) *Neurobiol. Dis.* **25,** 179–188
39. Aberle, H., Bauer, A., Stappert, J., Kispert, A., and Kemler, R. (1997) *EMBO J.* **16,** 3797–3804
40. Giuffrida, M. L., Caraci, F., Pignataro, B., Cataldo, S., De Bona, P., Bruno, V., Molinaro, G., Pappalardo, G., Messina, A., Palmigiano, A., Garozzo, D., Nicoletti, F., Rizzarelli, E., and Copani, A. (2009) *J. Neurosci.* **29,** 10582–10587
41. Lambert, M. P., Barlow, A. K., Chromy, B. A., Edwards, C., Freed, R., Liosatos, M., Morgan, T. E., Rozovsky, I., Trommer, B., Viola, K. L., Wals, P., Zhang, C., Finch, C. E., Krafft, G. A., and Klein, W. L. (1998) *Proc. Natl. Acad. Sci. U.S.A.* **95,** 6448–6453
42. Xie, L., Helmerhorst, E., Taddei, K., Plewright, B., van Bronswijk, W., and Martins, R. (2002) *J. Neurosci.* **22,** 221RC
43. Ma, Q. L., Yang, F., Rosario, E. R., Ubeda, O. J., Beech, W., Gant, D. J., Chen, P. P., Hudspeth, B., Chen, C., Zhao, Y., Vinters, H. V., Frautschy, S. A., and Cole, G. M. (2009) *J. Neurosci.* **29,** 9078–9089
44. Engel, T., Hernández, F., Avila, J., and Lucas, J. J. (2006) *J. Neurosci.* **26,** 5083–5090
45. Su, Y., Ryder, J., Li, B., Wu, X., Fox, N., Solenberg, P., Brune, K., Paul, S., Zhou, Y., Liu, F., and Ni, B. (2004) *Biochemistry* **43,** 6899–6908
46. Rockenstein, E., Torrance, M., Adame, A., Mante, M., Bar-on, P., Rose, J. B., Crews, L., and Masliah, E. (2007) *J. Neurosci.* **27,** 1981–1991
47. Noble, W., Planel, E., Zehr, C., Olm, V., Meyerson, J., Suleman, F., Gaynor, K., Wang, L., LaFrancois, J., Feinstein, B., Burns, M., Krishnamurthy, P., Wen, Y., Bhat, R., Lewis, J., Dickson, D., and Duff, K. (2005) *Proc. Natl. Acad. Sci. U.S.A.* **102,** 6990–6995
48. Masliah, E., Westland, C. E., Rockenstein, E. M., Abraham, C. R., Mallory, M., Veinberg, I., Sheldon, E., and Mucke, L. (1997) *Neuroscience* **78,** 135–146
49. Malm, T. M., Iivonen, H., Goldsteins, G., Keksa-Goldsteine, V., Ahtoniemi, T., Kanninen, K., Salminen, A., Auriola, S., Van Groen, T., Tanila, H., and Koistinaho, J. (2007) *J. Neurosci.* **27,** 3712–3721
50. Terwel, D., Muyllaert, D., Dewachter, I., Borghgraef, P., Croes, S., Devijver, H., and Van Leuven, F. (2008) *Am. J. Pathol.* **172,** 786–798
51. Kojro, E., Postina, R., Buro, C., Meiringer, C., Gehrig-Burger, K., and Fahrenholz, F. (2006) *FASEB J.* **20,** 512–514
52. Townsend, M., Mehta, T., and Selkoe, D. J. (2007) *J. Biol. Chem.* **282,** 33305–33312
53. Zhao, W. Q., Lacor, P. N., Chen, H., Lambert, M. P., Quon, M. J., Krafft, G. A., and Klein, W. L. (2009) *J. Biol. Chem.* **284,** 18742–18753
54. Decker, H., Jürgensen, S., Adrover, M. F., Brito-Moreira, J., Bomfim, T. R., Klein, W. L., Epstein, A. L., De Felice, F. G., Jerusalinsky, D., and Ferreira, S. T. (2010) *J. Neurochem.* **115,** 1520–1529
55. Knowles, J. K., Rajadas, J., Nguyen, T. V., Yang, T., LeMieux, M. C., Vander Griend, L., Ishikawa, C., Massa, S. M., Wyss-Coray, T., and Longo, F. M. (2009) *J. Neurosci.* **29,** 10627–10637
56. Capsoni, S., Giannotta, S., and Cattaneo, A. (2002) *Mol. Cell. Neurosci.* **21,** 15–28
57. Houeland, G., Romani, A., Marchetti, C., Amato, G., Capsoni, S., Cattaneo, A., and Marie, H. (2010) *J. Neurosci.* **30,** 13089–13094
58. Braithwaite, S. P., Schmid, R. S., He, D. N., Sung, M. L., Cho, S., Resnick, L., Monaghan, M. M., Hirst, W. D., Essrich, C., Reinhart, P. H., and Lo, D. C. (2010) *Neurobiol. Dis.* **39,** 311–317
59. Baglietto-Vargas, D., Moreno-Gonzalez, I., Sanchez-Varo, R., Jimenez, S., Trujillo-Estrada, L., Sanchez-Mejias, E., Torres, M., Romero-Acebal, M., Ruano, D., Vizuete, M., Vitorica, J., and Gutierrez, A. (2010) *J. Alzheimer Dis.* **21,** 119–132
60. Moreno-Gonzalez, I., Baglietto-Vargas, D., Sanchez-Varo, R., Jimenez, S., Trujillo-Estrada, L., Sanchez-Mejias, E., Del Rio, J. C., Torres, M., Romero-Acebal, M., Ruano, D., Vizuete, M., Vitorica, J., and Gutierrez, A. (2009) *J. Alzheimer Dis.* **18,** 755–776
61. Sotthibundhu, A., Sykes, A. M., Fox, B., Underwood, C. K., Thangnipon, W., and Coulson, E. J. (2008) *J. Neurosci.* **28,** 3941–3946
62. Ruano, D., Vizuete, M., Cano, J., Machado, A., and Vitorica, J. (1992) *J. Neurochem.* **58,** 485–493